New Wireless Power Transfer via Magnetic Resonant Coupling for Charging Moving Electric Vehicle

Koh Kim Ean[1)] **Takehiro Imura**[2)] **Yoichi Hori**[3)]
1) The University of Tokyo, Graduate School of Engineering
7-3-1 Hongo, Bunkyo, Tokyo, 113-8656 Japan (E-mail: koh@hori.k.u-tokyo.ac.jp)
2) 3) The University of Tokyo, Graduate School of Frontier Sciences
5-1-5, Kashiwanoha, Kashiwa, Chiba, 277-8561, Japan 277-8561

Presented at the EVTeC and APE Japan on May 22, 2014

ABSTRACT: New configuration for charging moving electric vehicle is proposed in this paper. Multiple transmitters are connected in parallel to a common power supply. When the electric vehicle departs from the transmitter, switching must be applied to ensure the branch is turned off when there is no load. Moreover, multiple small loop coils are preferred compared to a long loop coils to reduce power loss. Real time fast switching is needed when vehicles are moving on small charging loop coils. A repeater coil that is embedded under the road but above the transmitter is proposed. During no load condition, the branch becomes high impedance and only small current is pulled from the power supply. Switches are therefore only optional for emergency purpose or for turning off when there is no load for long time. Design equations for coupling and load impedance are also derived.

KEY WORDS: wireless power transfer, magnetic resonant coupling, electric vehicles, repeater coils

I. Introduction

Using wireless charging for electric vehicle is safe and convenient compared to plugging the vehicle into power outlet. Furthermore newly introduced wireless power transfer method that is magnetic resonant coupling increases the transferable distance and robustness to positional shift compared to magnetic induction method. This mid-range transfer method also enables charging while the vehicle is moving on the road.

The resonators can be embedded beneath and arranged along the road. Power is transferred through a series of coupled repeaters. Current is flowing in all the coils when charging which will cause increased dissipation loss. On the other hand, power received by a specified vehicles depends not only to own load impedance and coupling to the repeater but also other vehicles in the system [1]. Another disavantage of this repeater configuration is “dead zones” occur in certain positions where the power do not transfer to the load [2][3].

Charging moving electric vehicles has been proposed by [4][5]. Multiple segments are powered by rectifiers with shared inverters and only one segment can be turned on at a time. Sensors are implemented to turn off segments when there is no vehicles. In [6], a new rail configuration is proposed by changing the current direction to add up generated flux during activation mode or flux cancellation during silent mode. Multiple sub-rails activation is possible however real-time switching operations is required.

An analysis for comparing different sizes of transmitter coil is conducted by [7]. For different traffic conditions, small spaced loop coils have higher efficiency due to continuous turned on is not required. However using individual power supply for each small loop coil is expensive [4]. Therefore a new configuration for charging moving electric vehicle is proposed in this paper. Multiple transmitters are connected in parallel to a common power supply. However when the vehicles leaves each parallel branch, the branch becomes low impedance and high current that may damage the system is pulled from the supply. In order to avoid the dangerous no load condition without the need of fast real time switching, a repeater coil that is embedded under the road but above the transmitter is proposed so that only low current flow when the vehicle moves away.

II. Method

In addition to parallel connection, repeater coils in between transmitter and receiver as shown in Fig. 1 is also proposed. Without the repeater coils, each parallel branch would consist of only the resonant transmitter coil during no-load condition. The low internal impedance of the resonant transmitter coil will short-circuit the power supply if there is no switching implemented. In this configuration, the parallel branch becomes high impedance during no-load condition and only low current is pulled from the power supply. In this case, switch in individual branch is optional. Small loop coils with shared power supply can therefore be easily implemented as fast switching is no longer required. The repeater does not have to be above the transmitter in each parallel branch. The design is effective as long as the repeater is coupled to the transmitter and able to coupled to the receiver when the vehicle is approaching. Since the transmitter is required only to coupled to the repeater, the

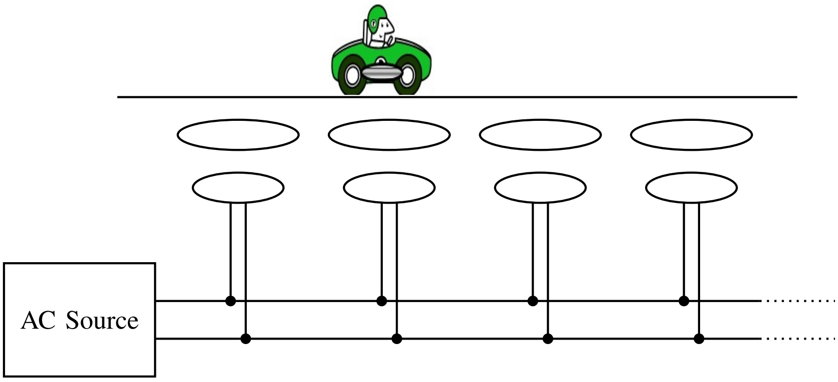

Fig. 1. Proposed configuration - middle repeater coils.

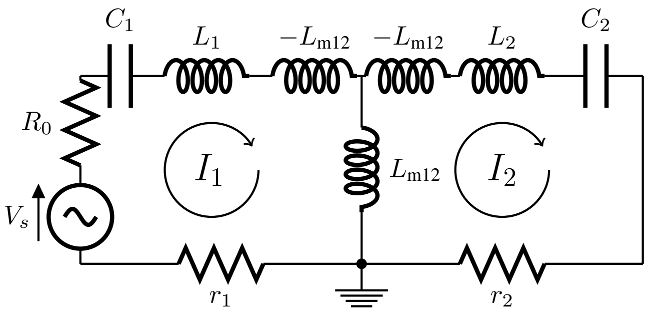

Fig. 2. Equivalent circuit for no-load branch

transmitter can be built smaller or even placed inside the bigger repeater. The only constraint is the transmitter should not coupled to the receiver.

Formulas during no-load condition and loaded condition are derived in this section to find a suitable coupling between transmitter and repeater.

A. No-load condition

Each parallel branch is considered separately to derive the design equation. Firstly, no-load condition is considered for one of the parallel branch. Equivalent circuit of a no-load branch is shown in Fig. 2. The current loop equations are given as:

$$\begin{aligned} V_s &= I_1(R_0 + Z_1) - I_2 j\omega_0 L_{m12} \\ 0 &= I_2 Z_2 - I_1 j\omega_0 L_{m12} \end{aligned} \tag{1}$$

and

$$\begin{aligned} Z_1 &= r_1 + j(\omega_0 L_1 - \frac{1}{\omega_0 C_1}) \\ Z_2 &= r_2 + j(\omega_0 L_2 - \frac{1}{\omega_0 C_2}) \end{aligned} \tag{2}$$

Where ω_0 is the resonant angular frequency and R_0 is the power supply internal impedance. Term r_1 and r_2 are the internal resistance of the transmitter and the repeater respectively whereas Z_1 and Z_2 are the impedance sum of the inductor, capacitor and internal resistance. In equivalent circuit, internal resistance is modelled in series with the inductor and capacitor [8]. Let:

$$K_{12} = \omega_0 L_{m12} \tag{3}$$

where K_{12} is the impedance inverter representation of coupling. As coupling coefficient k_{12} is [9]:

$$k_{12} = \frac{L_{m12}}{\sqrt{L_1 L_2}} \tag{4}$$

Impedance inverter representation can be related to coupling coefficient:

$$K_{12} = \omega_0 k_{12} \sqrt{L_1 L_2} \tag{5}$$

Impedance inverter representation will be used in the design equations to simplify the analysis [1].

Rearranging (1) and substituting (3), we obtain:

$$\begin{aligned} I_1 &= \frac{V_s}{R_0 + Z_1 + \frac{K_{12}^2}{Z_2}} \\ I_2 &= \frac{jK_{12}}{Z_2} I_1 \end{aligned} \tag{6}$$

Where I_1 and I_2 are transmitter current and repeater current respectively. Since Z_2 is the internal impedance of the resonant coil and is small, we can assume:

$$Z_1 \ll R_0 + \frac{{K_{12}}^2}{Z_2} \tag{7}$$

Transmitter current and repeater current are approximately:

$$\begin{aligned} I_1 &\approx \frac{V_s}{R_0 + \frac{{K_{12}}^2}{Z_2}} \\ I_2 &\approx \frac{jV_s \times K_{12}}{{K_{12}}^2 + R_0 Z_2} \end{aligned} \tag{8}$$

For low current flow in no-load branch, a large coupling between transmitter and repeater, K_{12} or equivalently large mutual inductance, L_{m12} can be chosen.

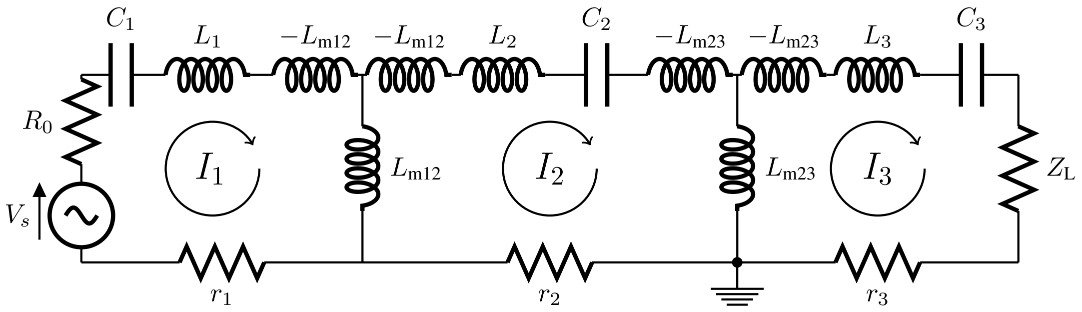

Fig. 3. Equivalent circuit for loaded branch.

B. Loaded condition

When a vechicle arrives above the parallel branch and begin charging, the equivalent circuit now becomes as in Fig. 3. The current loop equations:

$$\begin{aligned} V_s &= I_1(R_0 + Z_1) - I_2 j\omega_0 L_{\mathrm{m12}} \\ 0 &= I_2 Z_2 - I_1 j\omega_0 L_{\mathrm{m12}} - I_3 j\omega_0 L_{\mathrm{m23}} \\ 0 &= I_3(Z_{\mathrm{L}} + Z_3) - I_2 j\omega_0 L_{\mathrm{m23}} \end{aligned} \tag{9}$$

Where:

$$Z_3 = r_3 + j(\omega_0 L_3 - \frac{1}{\omega_0 C_3}) \tag{10}$$

Term Z_{L} is the load impedance, r_3 is the internal resistance of the receiver coil whereas Z_3 is the impedance sum of the inductor, capacitor and internal resistance. Similar to no-load condition, we let:

$$K_{23} = \omega_0 L_{\mathrm{m23}} \tag{11}$$

and:

$$k_{23} = \frac{L_{\mathrm{m23}}}{\sqrt{L_2 L_3}} \tag{12}$$

and rearranging (9), the current in transmitter, I_1, repeater, I_2 and receiver I_3 during loaded condition:

$$\begin{aligned} I_1 &= \frac{V_s}{Z_1 + R_0 + \frac{K_{12}{}^2}{Z_2 + \frac{K_{23}{}^2}{Z_3 + Z_{\mathrm{L}}}}} \\ I_2 &= \frac{jK_{12}}{Z_2 + \frac{K_{23}{}^2}{Z_3 + Z_{\mathrm{L}}}} I_1 \\ I_3 &= \frac{jK_{23}}{Z_3 + Z_{\mathrm{L}}} I_2 \end{aligned} \tag{13}$$

Assuming:

$$\begin{aligned} Z_3 &\ll Z_{\mathrm{L}} \\ Z_2 &\ll \frac{K_{23}{}^2}{Z_{\mathrm{L}}}. \end{aligned} \tag{14}$$

The approximated current during loaded condition:

$$\begin{aligned} I_1 &\approx \frac{V_s \times K_{23}{}^2}{K_{23}{}^2(R_0 + Z_1) + K_{12}{}^2 Z_{\mathrm{L}}} \\ I_2 &\approx \frac{V_s \times jK_{12} \times Z_{\mathrm{L}}}{K_{23}{}^2(R_0 + Z_1) + K_{12}{}^2 Z_{\mathrm{L}}} \\ I_3 &\approx \frac{-V_s \times K_{23} \times K_{12}}{K_{23}{}^2(R_0 + Z_1) + K_{12}{}^2 Z_{\mathrm{L}}}. \end{aligned} \tag{15}$$

Power received by the load:

$$P_{\mathrm{L}} \approx |\frac{-V_s \times K_{23} \times K_{12}}{K_{23}{}^2(R_0 + Z_1) + K_{12}{}^2 Z_{\mathrm{L}}}|^2 \times Re(Z_{\mathrm{L}}). \tag{16}$$

III. Simulation Results

The proposed configuration is simulated with $K_{12} = 43\,\Omega$, $85\,\Omega$, $128\,\Omega$ corresponding to $k_{12} = 0.05$, 0.1, 0.15 respectively to compare the efficiency of different K_{12}. Other parameters of the power transfer system:

$$\begin{aligned} V_s &= 300\,\mathrm{V} \\ Z_{\mathrm{L}} &= 25\,\Omega \\ R_0 &= 5\,\Omega \\ \omega_0 &= 2\pi \times 13.56\,\mathrm{MHz} \\ L_1 &= L_2 = L_3 = 10\,\mu\mathrm{H} \\ C_1 &= C_2 = C_3 = 13.8\,\mathrm{pF} \\ r_1 &= r_2 = r_3 = 1\,\Omega \end{aligned} \tag{17}$$

Simulation circuit shown in Fig. 4 with four identical parallel branches is inputted in LTspice where only the first branch is loaded. The coupling k_{23} of the receiver to the repeater of the loaded branch is varied from 0 to 0.1 to simulate a vehicle approaching one of the branch and moving towards maximum coupling point. Since large gap is more desirable, small receiver coupling is assumed in the real scenario. In this simulation, maximum coupling of receiver with each branch is 0.1. The arrangement of each branch is far enough so that cross coupling does not occur. Dissipation loss in each branch and power received are then calculated and compared.

Since the branches are identical, the power loss in each unloaded branch is the same. Fig. 5 shows the plot of power dissipated in each unloaded branch, loaded branch, power received by the load and transfer efficiency when the vehicle is approaching one of the branch from far until arriving at the point that has maximum coupling with the repeater of the branch. Efficiency plot in Fig. 5(d) is calculated through power received divided by sum of power received and loss in all parallel branches. Loss in the power supply is not considered in the efficiency calculation.

IV. Discussion

From (8) and plot in Fig. 5(a), stronger transmitter and repeater coupling, k_{12} reduces the unloaded power dissipation. However higher receiver to repeater coupling, k_{23} is

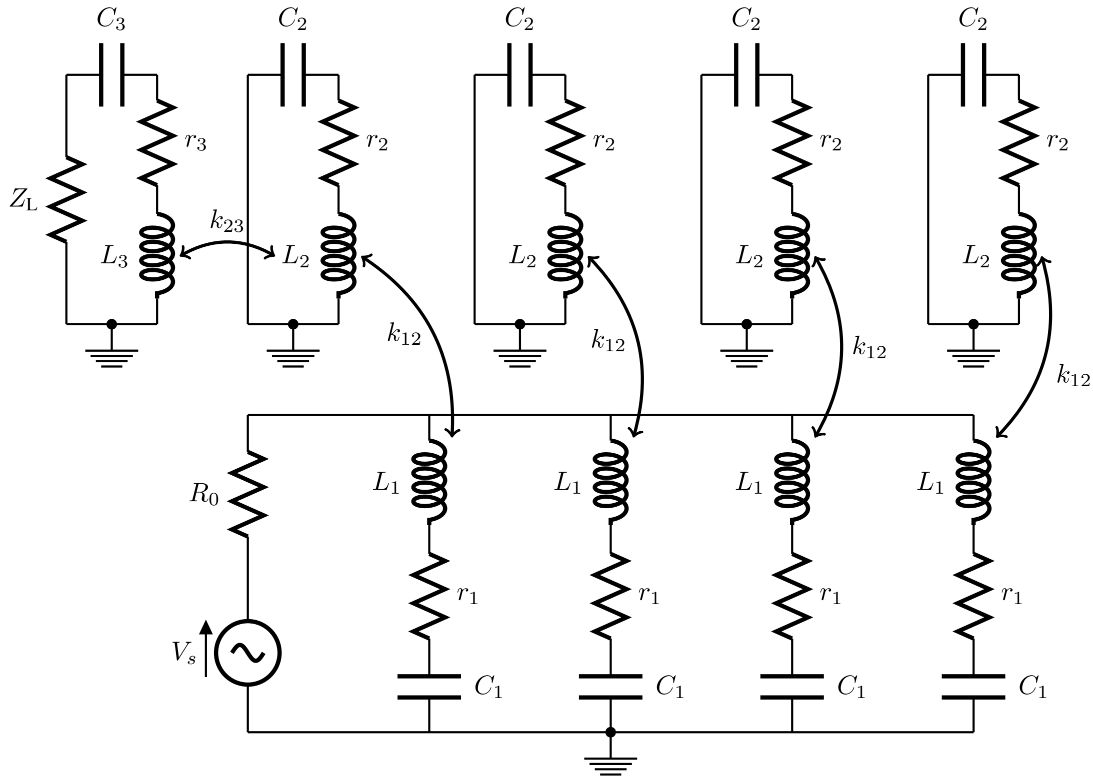

Fig. 4. Simulation circuit

needed to deliver same amount of power with high k_{12} when $(R_0 + Z_1) < Z_{\mathrm{L}}$ according to (16). Larger receiver gap is desirable as the underground wireless charging system can be burried deeper and thus is protected from the vibration on road. Therefore a better option is to reduce Z_{L} in this case. From (15), reducing Z_{L} also reduces transmitter current, i_1 while causes only small increase in repeater current, i_2 in loaded branch thus lower overall dissipation loss while maintaining the desired power level. For example if we change Z_{L} to $17.5\,\Omega$, and maintaining $k_{12} = 0.15$, we would obtain 2.2 kW for the load at point $k_{23} = 0.1$. The power loss in loaded branch and unloaded branch are respectively 132 W and 13 W. Comparing to point $k_{12} = k_{23} = 0.1$, where the power received is also around 2.2 kW, but the power loss in loaded branch and unloaded branch are respectively 182 W and 26 W.

Fig. 5(d) shows the efficiency plot at each coupling point. When the vehicle first arrives at the charging branch, coupling is small thus power received is also low. The low efficiency at these low coupling points is due to low power received divided by the disippation loss in unloaded branches that remains almost constant throughout the studied range. The power loss in unloaded branch is decreasing gradually when the load is getting closer for all designed k_{12}. This is due to the parallel impedance viewed from the source is decreasing when branches are loaded and this impedance is in series with the power supply impedance, R_0. Voltage division causes the voltage at each parallel branch to reduce and thus lower current flowing in the unloaded branch where the impedance does not change. If R_0 is zero, the voltage at each parallel branch would be constant. Also power received by each load will depend solely on the total impedance of the corresponding branch. Each parallel branch can be designed differently if needed, for example more power can be assigned to the charging spot near the traffic light by using lower tranmistter to repeater coupling with the expense of increased dissipation loss at that branch.

V. Conclusion

For different traffic conditions, small spaced loop coils have higher efficiency as continuous turn on of large loop coils are not required. However individual power supply for each coil is expensive. A new configuration is proposed where multiple transmitters are connected in parallel to share a power supply. By using parallel connection instead of a series of coupled repeaters, dead zone issue is eliminated. No-load condition will cause high current pulled from the supply and may damage the power transfer system. Fast switching is therefore necessary to avoid this condition when the load is moving. Proposed configuration also solves this issue by implementing a repeater coil above each transmitter. When load moves away, the parallel branch becomes high impedance and only small current will flow in the no-load branch.

Depending on the desired power level, gap between the vehicle's receiver to the repeater and power supply output impedance, the coupling between transmitter and repeater in each parallel branch and load impedance can be designed to obtain the optimised wireless power transfer system for charging moving electric vehicles.

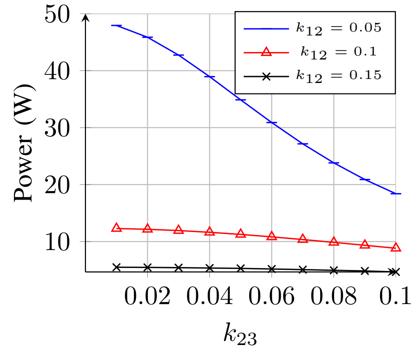

(a)

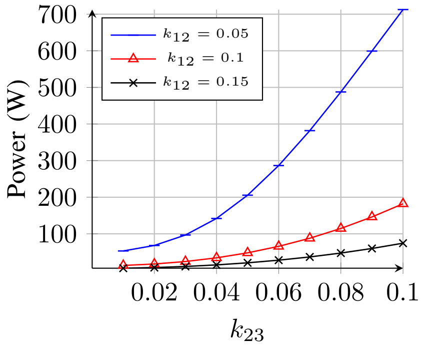

(b)

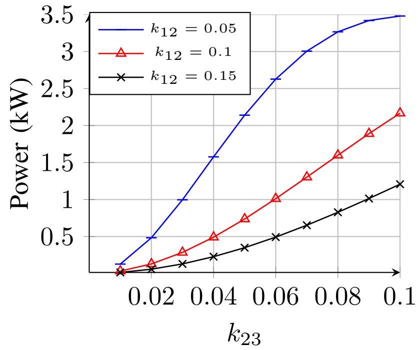

(c)

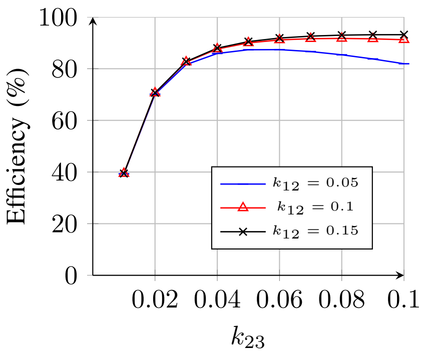

(d)

Fig. 5. Plot of a) power loss in each unloaded branch, b) power loss in loaded branch, c) power received vs coupling coefficient and d) transfer efficiency k_{23}.

REFERENCES

[1] K. E. Koh, T. C. Beh, T. Imura, Y. Hori., “Multi-receiver and repeater wireless power transfer via magnetic resonance coupling – impedance matching and power division utilizing impedance inverter,” The 15th Int. Conf. on Electrical Machines and Systems (ICEMS2012), 2012.

[2] J. W. Kim et al., “Wireless power transfer for free positioning using compact planar multiple self-resonators,” *2012 IEEE MTT-S Int. Microwave Workshop Series on Innovative Wireless Power Transmission: Technologies, Systems, and Applications (IMWS)*, pp. 127-130, May. 2012.

[3] Koh Kim Ean, Takehiro Imura, Yoichi Hori, “Impedance Inverter based Analysis of Wireless Power Transfer Consists of Repeaters via Magnetic Resonant Coupling”, *IEICE Technical Committee on Wireless Power Transmission (15th research seminar)*, Kanagawa, Japan, Dec. 2012.

[4] J. Shin et. al., “Design and implementation of shaped magnetic resonance based wireless power transfer system for roadway-powered moving electric vehicles,” *IEEE Trans. Ind. Electron.*, 2013.

[5] S. Shin et. al., “Hybrid inverter segmentation control for Online Electric Vehicle,” *2012 IEEE Int. Electric Vehicle Conference (IEVC).*

[6] S. Choi et. al., “New cross-segmented power supply rails for roadway-powered electric vehicles,” *IEEE Trans. Power Electron.*, Vol. 28, No. 12, pp. 5832-5841, Dec. 2013.

[7] M. Yilmaz, V. T. Buyukdegirmenci, and P. T. Krein, “General design requirements and analysis of roadbed inductive power transfer system for dynamic electric vehicle charging,” *2012 IEEE Transportation Electrification Conference and Expo (ITEC).*

[8] M. Dionigi and M. Mongiardo, “CAD of efficient wireless power transmission systems,” *IEEE MTT-S Int. Microwave Symp. Dig. (MTT)*, Jun. 2011, pp. 1-4.

[9] J. D. Irwin , R. M. Nelms, *Basic Engineering Circuit Analysis.* 10^{th} ed., NJ:John Wiley & Sons, Inc., 2010.